Available online at www.sciencedirect.com
ScienceDirect
Biochemical and Biophysical Research Communications 364 (2007) 40–47
BBRC
www.elsevier.com/locate/ybbrc

A role for Rab5 activity in the biogenesis of endosomal and lysosomal compartments

Yuko Hirota, Toshio Kuronita, Hideaki Fujita, Yoshitaka Tanaka *

Division of Pharmaceutical Cell Biology, Graduate School of Pharmaceutical Sciences, Kyushu University, 3-1-1 Maidashi, Fukuoka 812-8582, Japan

Received 20 September 2007
Available online 1 October 2007

Abstract

Rab5 is a small GTPase that plays roles in the homotypic fusion of early endosomes and regulation of intracellular vesicle transport. We show here that expression of GFP-tagged GTPase-deficient form of Rab5b (Rab5bQ79L) in NRK cells results in the sequential formation of three morphologically and functionally distinct types of endosomes. Expression of GFP-Rab5bQ79L initially caused a homotypic fusion of early endosomes accompanying a redistribution of the TGN-resident cargo molecules, and subsequent fusion with late endosomes/lysosomes, leading to the formation of giant hybrid organelles with features of early endosomes and late endosomes/lysosomes. Surprisingly, the giant endosomes gradually fragmented and shrunk, leading to the accumulation of early endosome clusters and concurrent reformation of late endosomes/lysosomes, a process accelerated by treatment with a phosphatidylinositol-3-kinase (PI(3)K) inhibitor, wortmannin. We postulate that such sequential processes reflect the biogenesis and maintenance of late endosomes/lysosomes, presumably via direct fusion with early endosomes and subsequent fission from hybrid organelles. Thus, our findings suggest a regulatory role for Rab5 in not only the early endocytic pathway, but also the late endocytic pathway, of membrane trafficking in coordination with PI(3)K activity.

Keywords: Rab5; Endosomes; Lysosomes; Ptdlns (3)-kinase; Wortmannin; Hybrid organelle; Lysosome biogenesis

Rab proteins constitute a subfamily of small GTPases that play important roles in the regulation of intracellular vesicle transport [1]. An intriguing early proposal was that different compartments in the exocytic and endocytic pathways contain distinct Rab GTPases on their surfaces [2]. Rab5 is the most thoroughly characterized member of the Rab GTPase family and is mainly localized to the early endosomal compartments [3]. It is now believed that Rab5 is essential for the homotypic fusion of early endosomes and is required for the endocytic pathways mediating the transport of clathrin-coated vesicles from the plasma membrane to the early endosomes [4,5].

There is less evidence to show that Rab5 affects the biogenesis of lysosomes. Lysosomes are dynamic organelles receiving materials from the biosynthetic, endocytic and autophagic pathways [6]. They are regarded as storage organelles for acid hydrolases and are capable for fusing with late endosomes to form hybrid organelles where the digestion of endocytosed macromolecules occurs. The reformation of lysosomes from the hybrid organelles involves a condensation of content and probably the removal of some membrane proteins by vesicular transport. Rosenfeld and colleagues [7] showed that lysosomal proteins were redistributed to endosomes during the expression of a GTPase-defective Rab5a (Rab5aQ79L) in macrophages. Little is known, however, about how the expression of Rab5aQ79L affects lysosome biogenesis. Therefore, in the present study we have investigated the involvement of Rab5 in the biogenesis and maintenance of late endosomes/lysosomes in more detail.

Materials and methods

Cell culture. Normal rat kidney (NRK), COS-1 and HeLa cells were cultured in Dulbecco's modified Eagle's medium (DMEM) supplemented

* Corresponding author. Fax: +81 92 642 6619.
E-mail address: tanakay@bioc.phar.kyushu-u.ac.jp (Y. Tanaka).

0006-291X/$ - see front matter © 2007 Elsevier Inc. All rights reserved.
doi:10.1016/j.bbrc.2007.09.089

with 10% (v/v) FBS (Gibco BRL, Grand Island, NY, USA), 2 mM glutamine and 1% penicillin–streptomycin in humidified 95% air and 5% CO_2 at 37 °C. The cells were plated onto 13 mm glass coverslips the day before infection.

DNA constructs. The cDNAs for human wild-type Rab5b and Rab5bQ79L inserted into the vector pCMV5-Flag [8] were subcloned in between the XhoI and HindIII sites of pEGFP-C1 (Clontech, Palo Alto, CA, USA).

Generation of adenoviruses. Adenoviruses encoding both Cre recombinase and GFP-Rab5bQ79L or GFP-Rab5b wild-type were generated as previously described [9]. We used Ψ5 as a donor to supply the viral backbone. The DNA sequence inserted between the Ψ site and the *loxP* site was incorporated into recombinant viruses in a Cre recombinase-catalyzed recombination between pAdlox and Ψ5. GFP-Rab5b was subcloned in between the KpnI and XbaI sites of pAdlox. GFP-Rab5bQ79L was subcloned in between the XbaI and EcoRI sites of pAdlox.

Adenoviral infection. NRK cells were infected with adenovirus for 6 h at 37 °C at a m.o.i. (multiplicity of infection) of 2×10^3 plaque-forming units/cell. After infection, the viral medium was removed, washed twice with medium, replaced with medium and chased for a given period.

Antibodies. Rabbit polyclonal antibodies to rat LGP85, rat MPR 300 and rat cathepsin D have been described [10–12]. Mouse monoclonal antibodies to EEA1, GM130, TGN38, syntaxin-6 and γ-adaptin were obtained from BD Transduction Laboratories (Lexington, KY, USA). Cy-3 or Cy-5-conjugated mouse monoclonal or rabbit polyclonal antibodies were purchased from Jackson ImmunoResearch Laboratories (West Grove, PA, USA).

Immunofluorescence microscopy. Cells cultured on glass coverslips were fixed in 4% paraformaldehyde and processed for immunofluorescence microscopy as described previously [13]. Confocal images were acquired using a Zeiss confocal microscope (LSM 510 META) equipped with an argon/HeNe laser and a ZEISS 100×/1.4 Plan-Apochromat oil immersion lens. All images were created using Adobe Photoshop CS (Adobe Systems, San Jose, CA).

Texas red-dextran internalization. One milligram per milliliter of Texas red-dextran (M_r, 70,000 lysine fixable) (Molecular Probes, Eugen, OR, USA) was added directly to the medium for 1 h, then cells were washed and fixed or incubated in medium for an additional 6 h before washing and fixation.

Results and discussion

GFP-Rab5bQ79L causes the sequential formation of three types of endosome differing in size and morphology

Previous studies from our laboratory and others suggested that Rab5 participates in the biogenesis of late endosomes/lysosomes as well as early endosomes [7,14]. In order to clarify the involvement of Rab5 in more detail, we carried out a time-course analysis of the expression of GFP-Rab5bQ79L. We used here an adenoviral infection system to achieve efficient and reproducible expression of GFP-Rab5bQ79L in NRK cells. An infection time of 6 h was sufficient to detect significant amounts of GFP-Rab5bQ79L in endosomal compartments using confocal laser microscopy. With this system, GFP-Rab5bQ79L was expressed in more than 80% of cells. Immediately after the infection for 6 h, GFP-Rab5bQ79L was seen as numerous small punctate structures throughout the cytoplasm (Fig. 1A-e), which were apparently larger than those seen in cells infected wild-type GFP-Rab5b adenovirus (Fig. 1A-a). After 2 h of chase, the number of small dot-like structures observed after infection decreased and instead relatively large ring-like vacuoles ~2 μm in size began to appear (Fig. 1A-f). The GFP-Rab5bQ79L-positive vacuoles were of maximal size (an average diameter of ~5 μm) after 6 h of chase (Fig. 1A-g). Interestingly, after 12 h of chase some cells expressing GFP-Rab5bQ79L had an unique structure with 5–10 small ring-like vacuoles, resembling "a bunch of grapes" (Fig. 1A-h). Such structures were not seen in cells chased for up to 6 h. The suggestion that such morphological changes depend on the chase time rather than on the expression level of GFP-Rab5bQ79L was supported by Western blot analysis, which showed that there was little change in the expression levels of GFP-Rab5bQ79L during 12 h of chase (data not shown). Based on the size and morphology of vacuoles induced by the expression of GFP-Rab5bQ79L, we categorized these GFP-Rab5bQ79L-positive compartments into three types (Fig. 1B); type I: the small endosomes (<2 μm) observed primarily in cells chased for 0 or 2 h (Fig. 1A-e and f), type II: the giant endosomes (about 5 μm) seen in half of the cells expressing GFP-Rab5bQ79L chased for 6 h (Fig. 1A-g) or type III: the clustered endosomes (about 1–2 μm), the number of which increased significantly when cells were chased for 12 h (Fig. 1A-h). Thus morphological changes observed during a series of chase periods were quantitated and revealed that cells expressing the clustered endosomes increase in number time-dependently, whereas the number of cells expressing the giant endosomes declined as the chase time increased (Fig. 1C). These results imply that the Rab5bQ79L-positive endosomes have been gradually transformed from type I to type III endosomes via type II. The same results were obtained in COS-1 and HeLa cells (Fig. 1A-i–p, D and E). In addition to the results that the formation of giant and clustered vacuoles was never seen in cells expressing wild-type GFP-Rab5b (Supplementary Fig. 2), GFP alone nor GFP-tagged dominant negative Rab5b (Rab5bS34N) (data not shown), the formation of these morphologically distinct endosomes was also caused by a transient transfection of Rab5bQ79L tagged with FLAG instead of GFP in COS cells (Supplementary Fig. 1), indicating a specificity for the expression of Rab5bQ79L, but not secondary effects due to the adenoviral infection and GFP tagged to Rab5bQ79L.

Next, we examined the involvement of organelles within the central vacuolar system in the morphological changes to Rab5bQ79L-positive endosomal compartments. The steady-state distribution of several well-characterized organelle markers did not affect in cells infected wild-type GFP-Rab5b adenovirus (Supplementary Fig. 2). EEA1 contains Rab5- and FYVE finger-binding domains in the C-terminus, which are necessary and sufficient for the recruitment of EEA1 to early endosomes [15,16]. Thus, the binding of EEA1 to endosomal membranes is required for both PI(3)K activity and Rab5-GTP [15]. As expected, EEA1 colocalized exclusively with all three types of GFP-Rab5bQ79L-positive vesicles (Fig. 2A–D-a). MPR300, which is a receptor for soluble lysosomal enzymes, mainly localizes in the TGN and rapidly recycles between the TGN

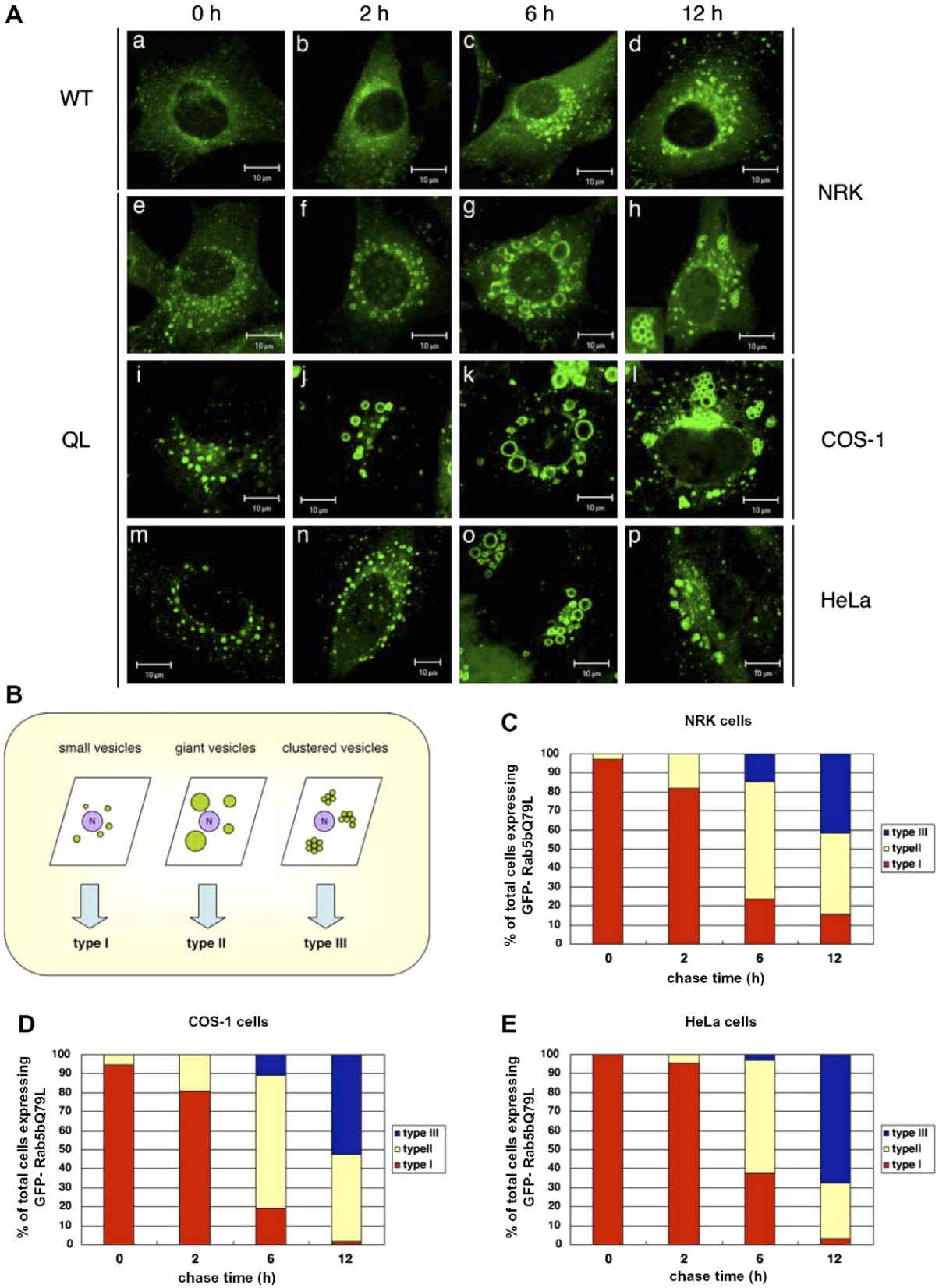

Fig. 1. The morphology of endosomes in cells overexpressing GFP-Rab5bQ79L or wild-type GFP-Rab5b. (A) NRK, COS-1 or HeLa cells were infected with adenovirus expressing GFP-Rab5bQ79L (e–p), or wild-type GFP-Rab5b (a–d) for 6 h, replaced with pre-warmed medium and then chased for the periods indicated at 37 °C prior to fixation. The bars represent 10 μm. (B) GFP-Rab5bQ79L-positive endosomes were categorized into three types based on diameter and morphology, as follows; type I: small vesicles of about 1–2 μm, type II: giant vesicles of about 5 μm or above, or type III: several clustered vesicles of about 1–2 μm. 'N' represents the nucleus. (C–E) NRK, COS-1 or HeLa cells were infected by the adenovirus expressing GFP-Rab5bQ79L for 6 h, chased for the periods indicated, and categorized into three types at each time based on counts of about 100 cells in 10 randomly chosen fields.

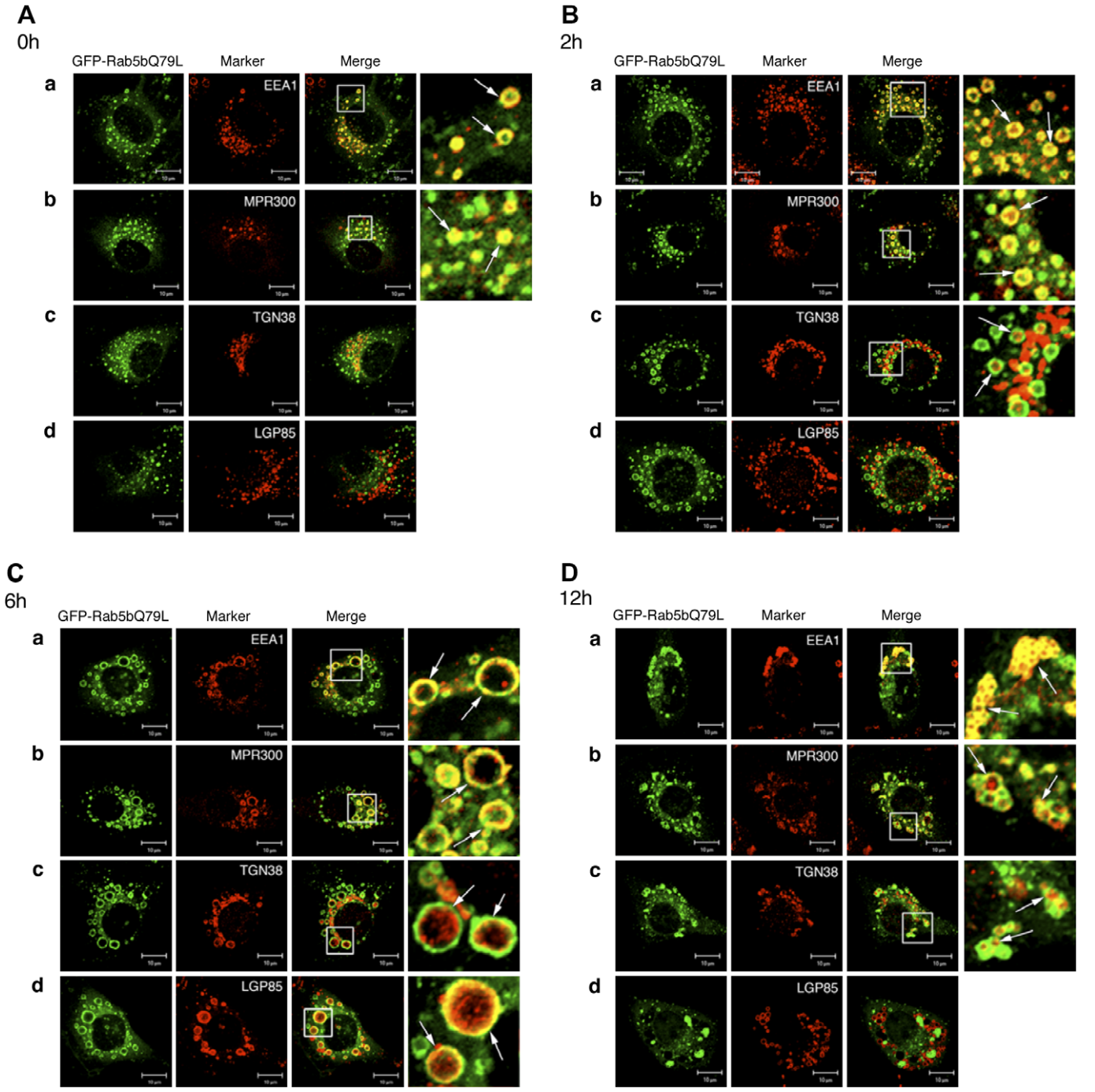

Fig. 2. Cytochemical characterization of the GFP-Rab5bQ79L-induced endosomal compartments. NRK cells infected with adenovirus expressing GFP-Rab5bQ79L for 6 h and chased for 0 (A), 2 (B), 6 (C) or 12 h (D) at 37 °C, were fixed and stained with antibodies for EEA1 (a), MPR300 (b), TGN38 (c), or LGP85 (d). Cells were then visualized by confocal microscopy. The colocalization of GFP-Rab5bQ79L (green) and each marker (red) is seen as yellow in the merged images. In the magnified images, the colocalization is indicated by arrows. The bars represent 10 μm.

and early endosomes [11,17]. The TGN-like staining pattern of MPR300 seen as reticular and small punctate structures around the perinuclear region in control cells (Supplementary Fig. 2B) was no longer observed in cells expressing GFP-Rab5bQ79L. Similar to EEA1, most of the MPR300 staining was seen in all types of GFP-Rab5bQ79L-positive vacuoles (Fig. 2A–D-b). It is suggested, therefore, that overexpression of GFP-Rab5bQ79L causes the redistribution of MPR300 from the TGN to early endosomes. On the other hand, TGN38, which is also transported between the TGN and cell surface via early endosomes [18,19], exhibited a somewhat different colocalization with GFP-Rab5bQ79L as compared with MPR300. In contrast to MPR300, the fine perinuclear reticular staining pattern of TGN38 seen in control cells (Supplementary Fig. 2E) did not change significantly in cells fixed

immediately after infection (Fig. 2A-c). After 2 h of chase, although most of the staining was still located in the TGN, a part was found in GFP-Rab5bQ79L-positive vacuoles (Fig. 2B-c). The fraction of TGN38 that colocalized with GFP-Rab5bQ79L increased as the chase got longer. Notably, the most dramatic effect of GFP-Rab5bQ79L expression on the localization of TGN38 was in the interior of GFP-Rab5bQ79L-positive enlarged type II endosomes (Fig. 2C-c). Although MPR300 was present in the limiting membranes of GFP-Rab5bQ79L-positive giant vacuoles (Fig. 2C-b), TGN38 was found only on the small vesicles within the giant vacuoles, often attached to the membranes (Fig. 2C-c). These results suggest that in contrast to MPR300, TGN38 may be sorted into vesicles that invaginate from the limiting membrane of endosomes. In contrast, the localization of the other TGN marker proteins, γ-adaptin and syntaxin-6, as well as the *cis*-Golgi marker protein GM130, was less affected by overexpression of GFP-Rab5bQ79L (Supplementary Fig. 3A–D-f, g). We further stained cells with antibodies to LGP85, which is an integral membrane glycoprotein of late endosomes and lysosomes [6]. In GFP-Rab5bQ79L-expressing cells chased for 0 or 2 h, the antibody to LGP85 stained numerous punctate structures, presumably corresponding to lysosomes, and was not significantly detected in the GFP-Rab5bQ79L-positive type I vesicles (Fig. 2A and B-d). Although after 6 h of chase, LGP85 was detected within the type II giant endosomes (Fig. 2C-d), it was never found in the clustered type III endosomes in cells chased for 12 h (Fig. 2D-d). Essentially, identical results were observed with antibody to a major soluble lysosomal enzyme cathepsin D (Supplementary Fig. 3). Interestingly, concomitant with the formation of GFP-Rab5bQ79L-positive type II endosomes, GFP-Rab5bQ79L-negative but LGP85- and cathepsin D-positive enlarged compartments were also formed, therefore, suggesting that the membrane trafficking from early endosomes is needed for the biogenesis and maintenance of late endosomes/lysosomes.

Late endosomes/lysosomes can reform from the type II giant hybrid organelles induced by Rab5bQ79L expression

We investigated the membrane trafficking from the Rab5bQ79L-positive endosomes to lysosomes using Texas-Red-conjugated dextran (TR-Dex). In uninfected cells, the majority of the internalized TR-Dex had already reached the late endosomes and/or lysosomes, as evidenced by colocalization with LGP85 (Fig. 3A). In cells chased for 2 h after the infection, most of the internalized TR-Dex was accumulated in LGP85-negative and GFP-Rab5bQ79L-positive compartments, i.e., early endosomes (Fig. 3B). Similarly, we observed the accumulation of TR-Dex in GFP-Rab5bQ79L- and LGP85-positive type II giant endosomes, but not in LGP85-positive and GFP-Rab5bQ79L-negative late endosomes/lysosomes (Fig. 3C). These results, therefore, suggest an impairment of transport from the GFP-Rab5bQ79L-positive type I or type II endosomes to lysosomes. On the other hand, cells expressing the type III clustered endosomes internalized little TR-Dex (Fig. 3D), suggesting that a fluid-phase endocytosis was impaired.

A very interesting result was obtained when cells expressing the type II giant endosomes were, being internalized TR-Dex, subsequently chased for 6 h. As would be expected, such an extended chase period after the infection led to an increase in the number of cells expressing the GFP-Rab5bQ79L-positive and LGP85-negative type III clustered endosomes and the concomitant formation of LGP85-positive and GFP-Rab5bQ79L-negative small vacuoles. We found that the internalized TR-Dex was no longer detectable in the GFP-Rab5bQ79L-positive type III clustered endosomes, and instead, colocalized exclusively with the GFP-Rab5bQ79L-negative and LGP85-positive vesicles (Fig. 3E). Moreover, at this time, although about 30–40% of GFP-Rab5bQ79L-expressing cells still exhibited the type II giant endosomes, the internalized TR-Dex remained in these giant endosomes without being delivered to the GFP-Rab5bQ79L-negative and LGP85-positive compartments (data not shown), suggesting that the trafficking of the internalized TR-Dex from the type II giant endosomes to lysosomes is severely impaired. Since most of the TR-Dex internalized in cells before a subsequent 6 h of chase was found in the GFP-Rab5bQ79L and LGP85-positive type II giant endosomes (Fig. 3C), these results suggest that the colocalization of the internalized TR-Dex with LGP85-positive compartments resulted from the reformation of late endosomes/lysosomes from the type II giant endosome–lysosomes hybrid organelles. It is conceivable, therefore, that the type II giant endosomes are gradually transformed into GFP-Rab5bQ79L-positive early endosome-like clustered vacuoles and to LGP85-positive late endosome/lysosome-like small vacuoles.

Wortmannin treatment accelerates the reformation of early endosomes and late endosomes/lysosomes from the type II giant endosomes

The docking and fusion between early endosomes, which are regulated by Rab5 [4,5], requires PI(3)K activity [1,2,10,16]. We then investigated whether the formation of three morphologically distinct types of endosomes induced by expression of Rab5bQ79L depends on the PI(3)K product phosphatidylinositol-3-phosphate (PtdIns(3)P). As expected, wortmannin caused an apparent decrease in the fluorescence signal for EEA1 (Supplementary Fig. 4E–H), reflecting the dissociation of EEA1 from the early endosomal membranes. The treatment with wortmannin of cells expressing the type I endosomes resulted in a slight enlargement of the GFP-Rab5bQ79L-positive type I vesicles relative to untreated cells, while most vesicles were EEA1-negative (Supplementary Fig. 4B, F). Additionally, LGP85-positive, but GFP-Rab5bQ79L-negative, structures were also slightly expanded by the wortmannin

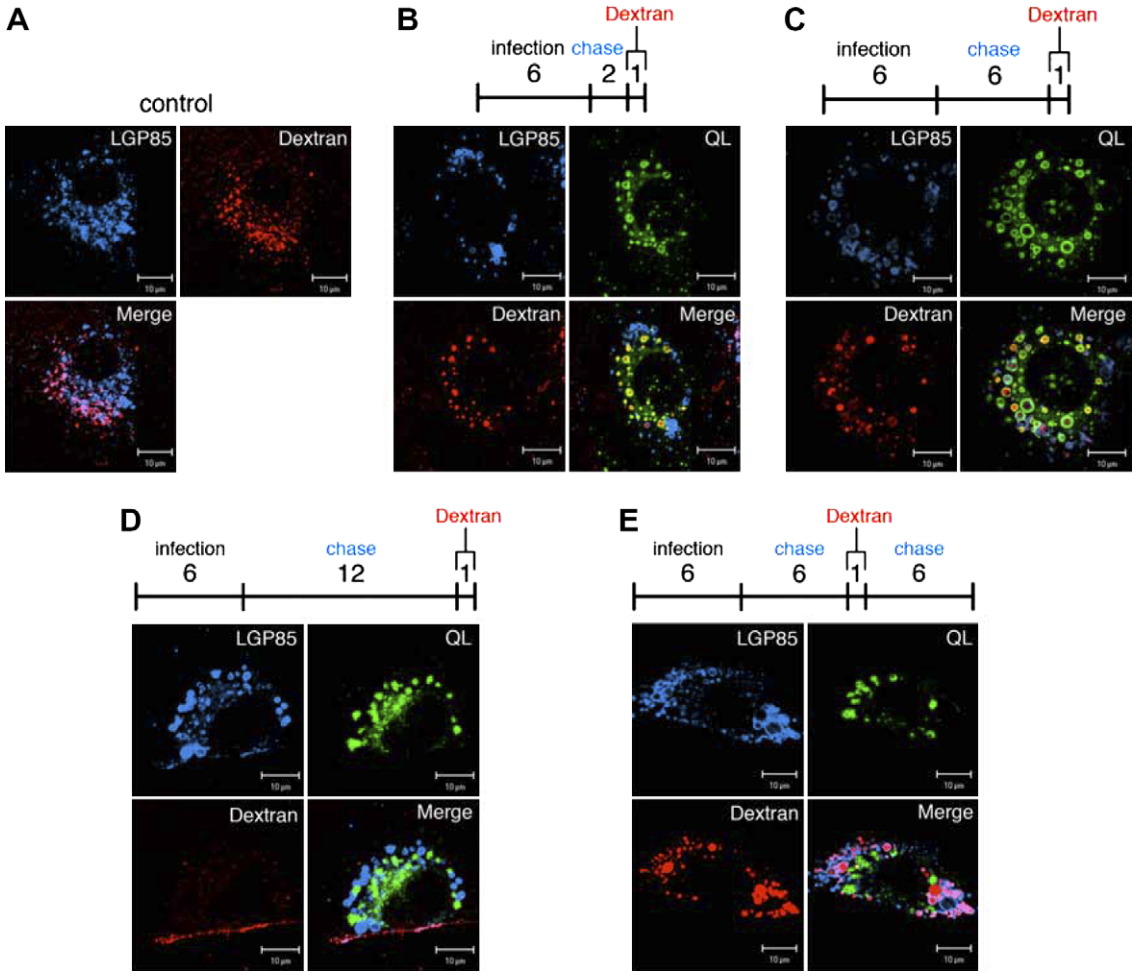

Fig. 3. Rab5bQ79L impairs transport from endosomes to lysosomes. Uninfected NRK cells (A) or GFP-Rab5bQ79L (green)-expressing NRK cells chased for 2 (B: type I), 6 (C: type II) or 12 h (D: type III) were fed TexasRed-dextran (red) for 1 h as described in Materials and methods. Cells were then fixed, stained with LGP85 (blue), and visualized by confocal microscopy. The type II cells that internalized dextran (C) were further chased for 6 h, fixed and stained for LGP85 (E). The bars represent 10 μm.

treatment. These results suggest that wortmannin stimulates the enlargement of early endosomes and late endosomes/lysosomes independently, despite the absence or presence of the GTP-bound form of Rab5 on their membranes. Surprisingly, when cells chased for 6 h after the infection were treated with wortmannin, the type II giant endosomes significantly disappeared. Instead, many GFP-Rab5bQ79L-positive small vesicles corresponding in size to the type I endosomes appeared throughout the cytoplasm, most of which were devoid of EEA1 and LGP85 (Supplementary Fig. 4C, G), indicating that wortmannin caused the reformation of early endosomes and late endosomes/lysosomes from the Rab5bQ79L and LGP85-positive type II giant endosomes. If this is the case, the internalized TR-Dex that accumulated in the type II giant endosomes would no longer be detected within the GFP-Rab5bQ79L-positive small endosomal compartments fragmented by the wortmannin treatment. Consistent with this prediction, the treatment with wortmannin of cells expressing TR-Dex-laden GFP-Rab5bQ79L-positive type II giant endosomes resulted in colocalization of TR-Dex with LGP85, but not with GFP-Rab5bQ79L in small vesicular structures (Fig. 4D–F). This effect was not observed in cells expressing TR-Dex containing type I endosomes (Fig. 4A–C). These results, therefore, suggest that the decrease in PtdIns(3)P from the type II giant endosomes may accelerate fission of vesicles and as a result, cause the reformation of early endosomes and late endosomes/lysosomes. On the other hand, when cells expressing the type III clustered endosomes were treated with wortmannin, there was no drastic morphological alteration of the endosomes compared with untreated cells, although the endosomes occasionally had a tendency to disperse slightly (Supplementary Fig. 4D, H), suggesting that the clustering of GFP-Rab5bQ79L-positive vacuoles may depend on PtdIns(3)P.

Conclusion

On the basis of the time-dependent appearance of three morphologically and functionally distinct endosomal compartments by Rab5bQ79L expression, we

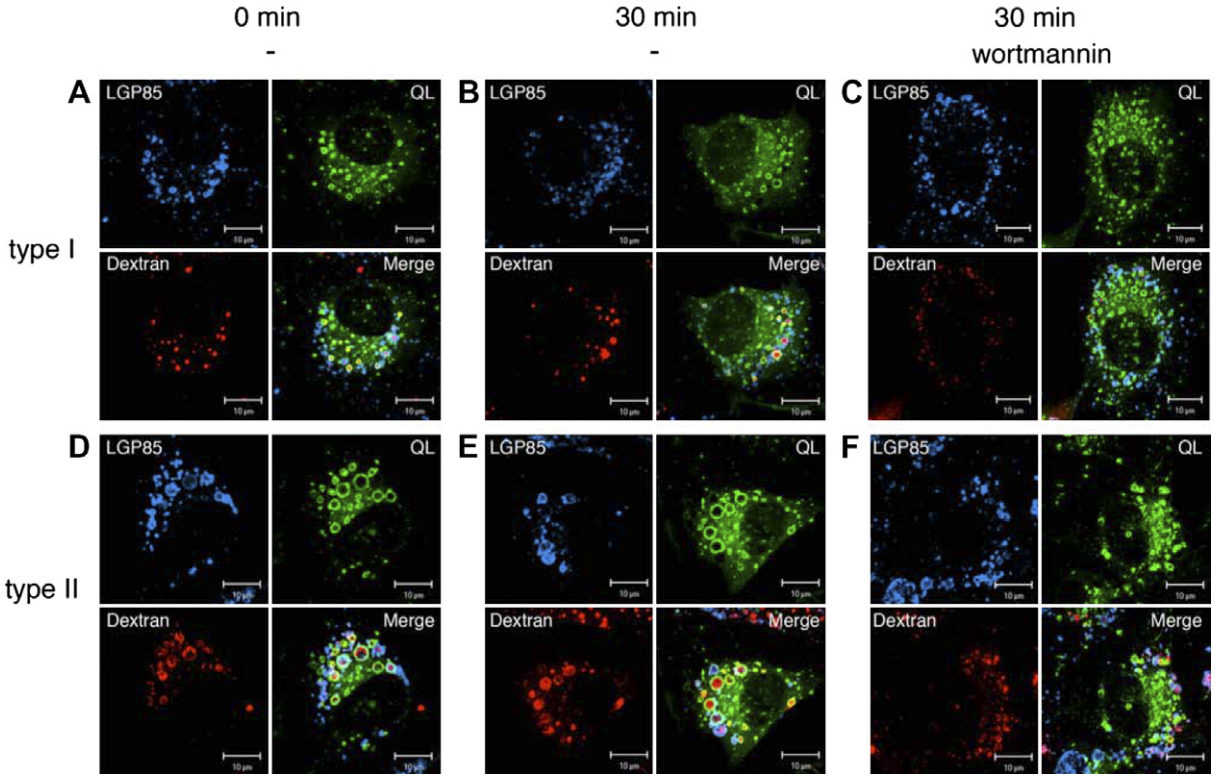

Fig. 4. Wortmannin causes the reformation of late endosomes/lysosomes from Rab5bQ79L-positive type II giant endosomes. GFP-Rab5bQ79L (green)-expressing NRK cells chased for 2 (A–C: type I), or 6 (D–F: type II) hours after the infection were fed TexasRed-dextran (red) for 1 h. Cells were then treated with 100 nM wortmannin (C, F) or left untreated (B, E) for 30 min at 37 °C, fixed and stained with a rabbit polyclonal antibody to LGP85 (blue). Cells were visualized by confocal microscopy. The bars represent 10 μm.

postulate that these endosomal compartments are formed sequentially in three steps. The first step, the formation of type I endosomes, is initiated by the homotypic fusion of early endosomes and simultaneous fusion with carrier vesicles derived from the TGN. The second step, the formation of type II giant endosomes, occurs via a subsequent fusion of the type I endosomes with late endosomes/lysosomes, displaying hybrid organelles composed of early endosomes, late endosomes and lysosomes as well as some cargo molecules that recycle between the TGN and early endosomes such as TGN38 and MPR300. The third step, the formation of type III clustered endosomes, seems to be caused by vesiculation of the type II giant endosomes. The surprising finding is that during the formation of the type III clustered endosomes from the type II giant endosomes, late endosomes/lysosomes also appeared to reform and detach from the clusters of early endosomes. Furthermore, the wortmannin treatment accelerated the fragmentation of the type II giant vacuoles accompanying the segregation of early endosomes and late endosomes/lysosomes without additional enlargement, suggesting a role of PtdIns(3)P in both the enlargement and subsequent clustering of early endosomes. Also, our results suggest the ability of endosomes to maintain organelle identity in the face of dysregulated endosomal fusion.

The time-dependent morphological changes of endosomal/lysosomal compartments caused by Rab5bQ79L expression may reflect the processes of the biogenesis of lysosomes, which occur through interaction between late endosomes and lysosomes by continuous transient fusion and fission [reviewed in [20]]. Recently, using time-lapse confocal microscopy in living cells, Bright et al. [21] demonstrated that direct fusion and transient exchange via kissing occur concurrently between late endosomes and lysosomes. Therefore, the ''fusion–fission'' and/or ''kiss-and-run'' hypothesis may explain the direct fusion between early endosomes and late endosomes/lysosomes (the formation of type II giant endosomes) and subsequent reformation of the respective compartment (the formation of type III endosomes and late endosomes/lysosomes) caused by overexpression of Rab5bQ79L.

The findings presented in this paper suggest that early endosomes have the capacity to fuse with late endosomes/lysosomes, which is promoted by expression of an active form of Rab5. Thus heterotypic fusion could occur constitutively, but might be difficult to detect as it is an extremely rapid process. Therefore, expression of Rab5bQ79L enabled us to detect sequential morphological changes, presumably reflecting the processes of lysosome biogenesis. Thus, our findings provide important new insights into the role of Rab5 in the biogenesis and mainte-

nance of late endosomes/lysosomes and their dynamic membrane exchange with early endosomes through coordinated action with PI(3)K.

Acknowledgments

We thank Drs. K. Saito and T. Katada (University of Tokyo) and L.T. Braiterman and A.L. Hubbard (Johns Hopkins University) for providing the Rab5b construct and adenovirus, respectively. This study was supported in part by a grant-in-aid from the Ministry of Education, Culture, Sports, Sciences and Technology of Japan. Y.H. is a Research Fellow of the Japan Society for the Promotion of Science.

Appendix A. Supplementary data

Supplementary data associated with this article can be found, in the online version, at doi:10.1016/j.bbrc.2007.09.089.

References

[1] M. Zerial, H. McBride, Rab proteins as membrane organizers, Nat. Rev. Mol. Cell Biol. 2 (2001) 107–117.
[2] J. Somsel Rodman, A. Wandinger-Ness, Rab GTPases coordinate endocytosis, J. Cell Sci. 113 (2000) 183–192.
[3] H. Stenmark, R.G. Parton, O. Steele-Mortimer, A. Lütcke, J. Gruenberg, M. Zerial, Inhibition of rab5 GTPase activity stimulates membrane fusion in endocytosis, EMBO J. 13 (1994) 1287–1296.
[4] J.P. Gorvel, P. Chavrier, M. Zerial, J. Gruenberg, Rab5 controls early endosome fusion in vitro, Cell 64 (1991) 915–925.
[5] C. Bucci, R.G. Parton, I.H. Mather, H. Stunnenberg, K. Simons, B. Hoflack, M. Zerial, The small GTPase rab5 functions as a regulatory factor in the early endocytic pathway, Cell 70 (1992) 715–728.
[6] E.L. Eskelinen, Y. Tanaka, P. Saftig, At the acidic edge: emerging functions for lysosomal membrane proteins, Trends Cell Biol. 13 (2003) 137–145.
[7] J.L. Rosenfeld, R. Moore, K.P. Zimmer, E. Alpizar-Foster, W. Dai, M.N. Zarka, B.J. Knoll, Lysosome proteins are redistributed during expression of GTP-hydrolysis-defective rab5a, J. Cell Sci. 114 (2001) 4499–4508.
[8] K. Kurosu, T. Katada, Association of phosphatidylinositol 3-kinase composed of p110β-catalytic and p85-regulatory subunits with the small GTPase Rab5, J. Biochem. 130 (2001) 73–78.
[9] S. Hardy, M. Kitamura, T. Harris-Stansil, Y. Dai, M.L. Phipps, Construction of adenovirus vectors through Cre-lox recombination, J. Viro. 71 (1997) 1842–1849.
[10] T. Kuronita, T. Hatano, A. Furuyama, Y. Hirota, N. Masuyama, P. Saftig, M. Himeno, H. Fujita, Y. Tanaka, The NH_2-terminal transmembrane and lumenal domains of LGP85 needed for the formation of enlarged endosomes/lysosomes, Traffic 6 (2005) 895–906.
[11] K. Hirosako, H. Imasato, Y. Hirota, T. Kuronita, N. Masuyama, M. Nishioka, A. Umeda, H. Fujita, M. Himeno, Y. Tanaka, 3-Methyladenine specifically inhibits retrograde transport of cation-independent mannose 6-phosphate/insulin-like growth factor II receptor from the early endosome to the TGN, Biochem. Biophys. Res. Commun. 316 (2004) 845–852.
[12] Y. Tanaka, G. Guhde, A. Suter, E.L. Eskelinen, D. Hartmann, R. Lüllmann-Rauch, P.M.L. Janssen, J. Blanz, K. von Figura, P. Saftig, Accumulation of autophagic vacuoles and cardiomyopathy in LAMP-2-deficient mice, Nature 406 (2000) 902–906.
[13] Y. Hirota, N. Masuyama, T. Kuronita, H. Fujita, M. Himeno, Y. Tanaka, Analysis of post-lysosomal compartments, Biochem. Biophys. Res. Commun. 314 (2004) 306–312.
[14] T. Kuronita, E.L. Eskelinen, H. Fujita, P. Saftig, M. Himeno, Y. Tanaka, A role for the lysosomal membrane protein LGP85 in the biogenesis and maintenance of endosomal and lysosomal morphology, J. Cell Sci. 115 (2002) 4117–4131.
[15] A. Simonsen, R. Lippe, S. Christoforidis, J.M. Gaullier, A. Brech, J. Callaghan, B.H. Toh, C. Murphy, M. Zerial, H. Stenmark, EEA1 links PI(3)K function to Rab5 regulation of endosome fusion, Nature 394 (1998) 494–498.
[16] S. Christoforidis, H.M. McBride, R.D. Burgoyne, M. Zerial, The Rab5 effector EEA1 is a core component of endosome docking, Nature 397 (1999) 621–625.
[17] A. Umeda, H. Fujita, T. Kuronita, K. Hirosako, M. Himeno, Y. Tanaka, Distribution and trafficking of MPR300 is normal in cells with cholesterol accumulated in late endocytic compartments: evidence for early endosome-to-TGN trafficking of MPR300, J. Lipid Res. 44 (2003) 1821–1832.
[18] B. Reaves, M. Horn, G. Banting, TGN38/41 recycles between the cell surface and the TGN: brefeldin A affects its rate of return to the TGN, Mol. Biol. Cell. 4 (1993) 93–105.
[19] G. Banting, S. Ponnambalam, TGN38 and its orthologues: roles in post-TGN vesicle formation and maintenance of TGN morphology, Biochim. Biophys. Acta 1355 (1997) 209–217.
[20] J.P. Luzio, V. Poupon, M.R. Lindsay, B.M. Mullock, R.C. Piper, P.R. Pryor, Membrane dynamics and the biogenesis of lysosomes, Mol. Memb. Biol. 20 (2003) 141–154.
[21] N.A. Bright, M.J. Gratian, J.P. Luzio, Endocytic delivery to lysosomes mediated by concurrent fusion and kissing events in living cells, Cur. Biol. 15 (2005) 360–365.